

EMC3-Eirene simulations of the spatial dependence of the tungsten divertor retention in the magnetically perturbed ASDEX Upgrade edge plasma

T. Lunt¹, Y. Feng¹, A. Janzer¹, P. de Marné¹, A. Herrmann¹, W. Suttrop¹

and the ASDEX Upgrade team

¹ Max-Planck-Institute für Plasmaphysik, Garching/Greifswald, Germany

1 Introduction

Magnetic perturbation (MP) coils are used in several tokamaks in the world (COMPASS, DIII-D, JET, Mast, ...) to suppress edge localized modes (ELMs), quasi-periodic expulsions of particles and energy from the edge plasma to the surrounding plasma facing components. Since December 2010 a new set of 8 in-vessel MP coils is operational also at ASDEX Upgrade (AUG), which has proven to suppress ELMs effectively. While a detailed description of a variety of experiments studying in particular the conditions for ELM suppression can be found in Ref. [1] here we analyze one particular discharge (characterized in Sec. 2).

In order to be able to make predictions for ITER, where the application of MP coils is also planned, a validated theoretical model to describe the edge plasma transport is highly desired. Since the MP coils break the toroidal symmetry of the tokamak, such a model has to take into account the full 3D geometry including the stochastic fields induced by the coils. Recently, the Edge Monte Carlo 3D (EMC3) - Eirene code package was implemented successfully at AUG and has been validated for limiter [2] and divertor discharges in the axi-symmetric configuration without MPs [3, 4]. In the near future we will report in detail on EMC3-Eirene simulations of the plasma edge transport presently carried out including the MP fields. Here we show part of these results with a focus on the simulated plasma profiles on the outer divertor target (Sec. 3), which are most important for the simulations of the impurity transport from a localized tungsten source at the target plate described in Sec. 4. These profiles show various maxima and minima in particular in the power deposition pattern, an effect also known as strike point splitting in the literature [5, 6]. The work presented in this article is thus a continuation Ref. [4] where a very sensitive dependency of the divertor retention to the source location was found for the axi-symmetric case. Sec. 5 finally gives a summary of the results.

2 Experiment

Fig. 1 shows the time traces of several parameters of AUG discharge 26081. During the entire flattop phase (1–7 s) the plasma current remains constant at $I_p = -800$ kA as seen in box (a). From 2–5.3 s a current of $I_{MP} = 4.5$ kAt is driven through the MP coils, which are connected in an odd parity $n = 2$ configuration. We will refer to this time period as the ‘MP phase’ in contrast to the ‘non-MP phase’ before. An important observation is that neither the line averaged density \bar{n}_e nor the stored energy W_{MHD} (black and red curves in box (b)) are reduced by the action of the MP fields. The first rather shows a slight increase than a ‘density pump-out’ as observed in other machines [5]. The ELMs, however, are effectively suppressed as seen in the data from divertor currents (box d) and also from the 1D infrared camera (box e). While ELMs deposit

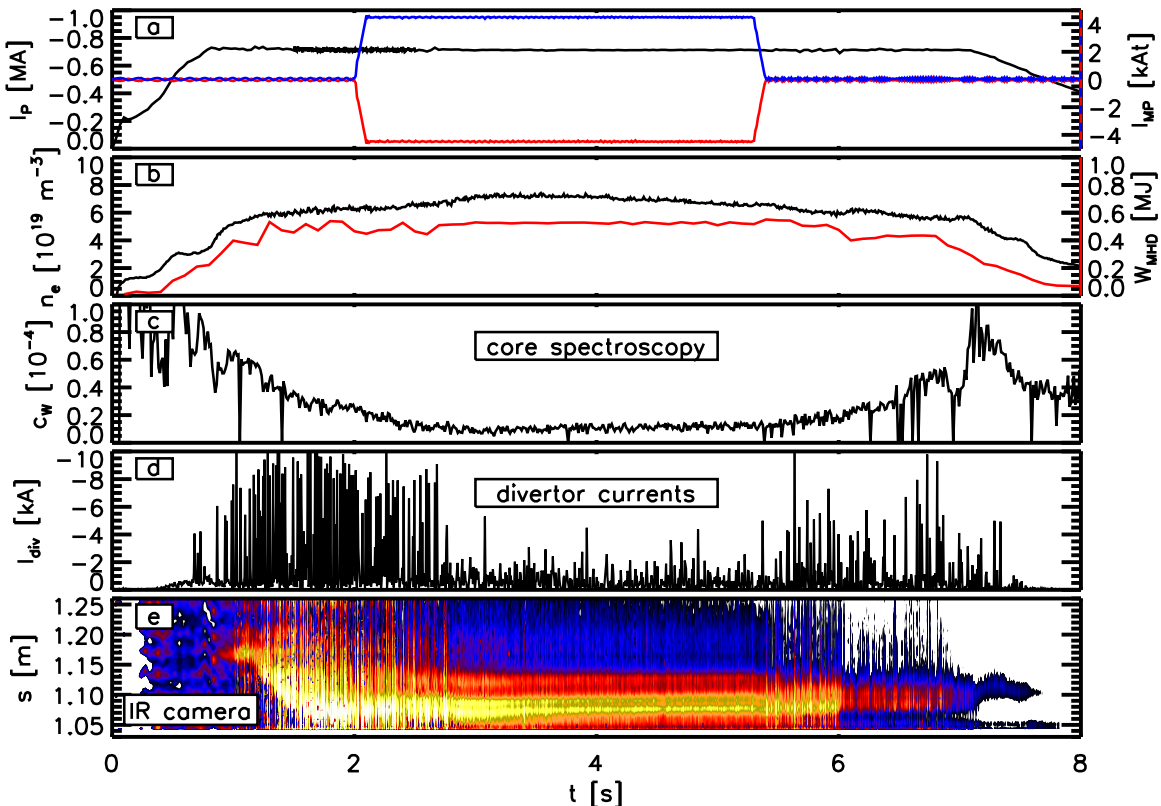


Figure 1: Time traces of selected parameters during AUG discharge 26081. The power deposition profiles (box e) are also shown in Fig. 2 for $t = 4.9$ s and $t = 1.9$ s respectively.

large amounts of particles and energy in frequent eruptions on a short time scale during the non-MP phase (scattered signals in boxes d and e from 1–2.5 s) the divertor currents become much smaller and the power deposition much smoother in the MP phase. In addition to that the power deposition profile shows clearly the aforementioned ‘strike-point splitting’ from 3 to 5 s. Despite the reduced ELM-activity it is also observed that during the MP phase the tungsten impurity concentration c_w measured by core spectroscopy (box c) is particularly low. This effect was observed even more clearly for AUG L-modes [7].

Other parameters that characterize the discharge are $B_t = -2.5$ T, $q_{95} = -5.7$ and $P_{in} = P_{NI} + P_{ECRH} + P_{OH} = 3.7 + 1.6 + 0.16$ MW = 9 MW. A significant fraction of the input power (5 MW or 56 %) is radiated by the neutral deuterium and different impurities outside the separatrix, while the rest is finally deposited on the divertor target plates.

3 Simulation of the bulk plasma

Assuming the experimental boundary conditions given in Sec. 2 and the magnetic fields computed from the equilibrium reconstruction and current loops in the MP coils (‘vacuum approach’) plasma parameters as well as neutral particle densities were computed by means of EMC3-Eirene for an entire toroidal period of 180°. In contrast to the axisymmetric non-MP case helical structures are clearly observed in the 3D results including the MP fields, in particular in the streaming velocity field (not shown here).

In order to fit as well as possible the main chamber n_e , T_e and T_i profiles measured by the Li-beam, the ECE diagnostics and charge exchange spectroscopy constant anomalous particle and heat diffusion coefficients of $D_{\perp} = 0.25 \text{ m}^2/\text{s}$ and $\chi_{\perp} = 2.5 \text{ m}^2/\text{s}$ and a separatrix density of $n_{e,sep} = 3.9 \cdot 10^{19} \text{ m}^{-3}$ were assumed. The simulated and the measured power flux deposited at the outer divertor target plate is shown in Fig. 2. Since impurity radiation was not yet taken into account in the simulation it is not surprising that the absolute value and the offset in measured power flux (red curves) are not yet in agreement with the simulation (black curve). A factor of about 5 difference, however, is rather high and has to be further investigated. Possibly the discrepancy is related to the quite inhomogeneous deposition pattern in toroidal direction due to the finite tilt angle of the tiles. Irrespective of this, the profile, which shows several maxima and minima for the MP case (Fig. 2 top) is quite well reproduced by the simulation. This strike-point splitting does not appear in both the simulation and the experiment in the non MP phase (Fig. 2 bottom), which confirms that the effect is actually caused by the action of the MP coils and not by any numerical or statistical error. The shift of the maxima between the red and black curves is most likely explained by inaccuracies in the equilibrium and/or the target geometry.

4 Impurity transport simulations

The impurity transport simulations described in this section are carried out in analogy with those in Ref. [4] but for the deuterium bulk plasma described in previous section. In Ref. [4] we introduced the mean tungsten residence time by $\tau_W = N_W/\Phi_W$, where N_W is the total number of tungsten atoms in the core for a given source of the strength Φ_W . The ratio

$$R = \frac{\tau_{W,mc}}{\tau_{W,div}}. \quad (1)$$

for a main chamber (mc) and a divertor (div) source is called ‘divertor retention’, as it was also defined by Roth and Janeschitz [8]. R is plotted in Fig. 3, where the case with (red and blue) and without (black) MPs are distinguished. Due to the toroidal asymmetry of the plasma two toroidal positions $\phi = 0^\circ$ (red) and $\phi = 90^\circ$ (blue) of the source are compared.

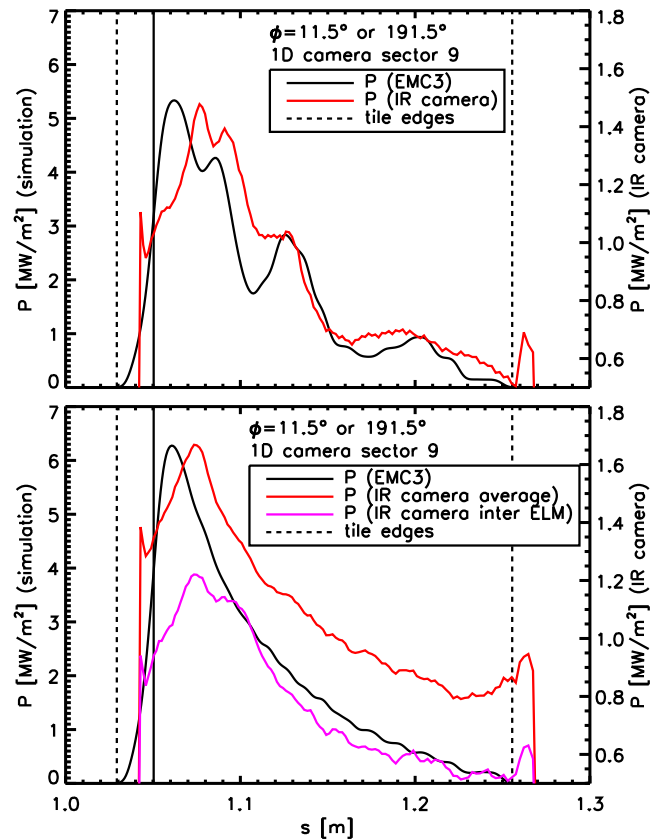


Figure 2: Power deposition profiles with (top) and without (bottom) magnetic perturbations.

In order to obtain the profiles the simulation is repeated 100 times while scanning the position of a source with a constant strength relative to the strike point. In Ref. [4] we have found that R correlates closely to the ratio n_e/T_i^2 , which apparently is also the case with MPs. As n_e slightly increases in the MP case, while T_i decreases, this explains why R is significantly higher for the MP case in particular in the region 20 mm above the strike point. Comparing the toroidally averaged deposition profiles of the MP case to those of the axisymmetric solution a slight broadening is noticed, which is associated with the enhancement of the radial transport induced by the MP fields. This effect, however, is relatively small and presently it is not yet clear, whether this is the only explanation. While a more refined quantitative analysis of the sources is still going on, the simulation results have shown the same trend as the aforementioned qualitative result that the tungsten concentration decreases when turning on the MP coils. One of the next steps will also be to increase the grid resolution at the target plate even further. The finite grid resolution seems to be responsible for an overestimation of the density (Fig. 3 middle), which was measured significantly smaller by the divertor Langmuir probes.

5 Summary

For the first time, non-axisymmetric divertor plasmas in AUG at the presence of magnetic perturbations (MPs) were simulated using the EMC3-Eirene code package. The ‘MP phase’ was compared to the ‘non MP phase’ as a reference. Although the measured absolute value for the power flux to the target differs by a factor of 5 from the simulation, the profiles, which show clearly a ‘strike point splitting’ are reproduced quite well by EMC3-Eirene. Additionally the impurity transport was simulated for a localized tungsten source in the divertor. These simulations clearly show an increase of the divertor retention due to the action of the MPs, which is in qualitative agreement with the experiment.

References

- [1] Suttrop W. *et al.* 2011 *Phys. Rev. Lett.* **106** 225004
- [2] Lunt T. *et al.* 2009 36th EPS Conference on Plasma Phys., Sofia, Bulgaria, P-1.154
- [3] Lunt T. *et al.* 2011 accepted for publication in *J. Nucl. Mater.*
- [4] Lunt T. *et al.* 2011 submitted to *Plasma Phys. Control. Fusion*
- [5] Schmitz O. *et al.* 2008 *Plasma Phys. Control. Fusion* **50** 124029
- [6] Frerichs H. *et al.* 2010 *Nucl. Fusion* **50** 034004
- [7] Weller A. *et al.* 2011 38th EPS Conference on Plasma Phys., Strasbourg, France, P-5.054
- [8] Roth J. and Janeschitz G. 1989 *Nucl. Fusion* **29** No.6 915–935

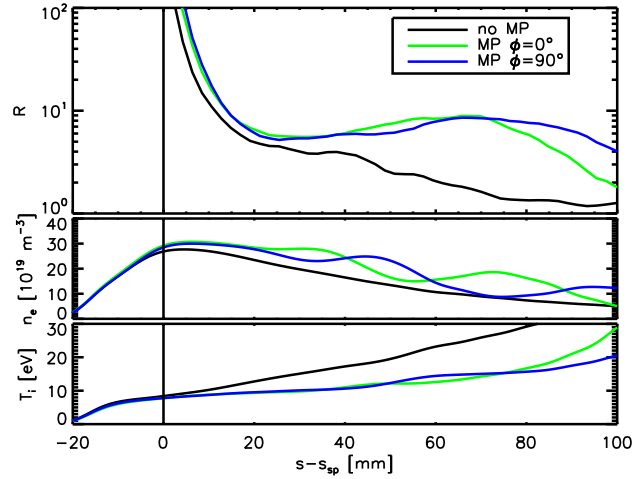


Figure 3: Top: divertor retention as a function of spatial distance $s - s_{sp}$ to the outer strike point. Middle and bottom: n_e and T_i at the outer target plate.